ISSN: 1648-6897 / eISSN: 1822-4199

VILNIUS TECH
Vilnius Gediminas Technical University

JOURNAL of ENVIRONMENTAL ENGINEERING & LANDSCAPE MANAGEMENT

2024
Volume 32
Issue 4
Pages 270–282
https://doi.org/10.3846/jeelm.2024.22352

TEMPERATURE AND PRECIPITATION PROJECTION IN THE LOWER MAHANADI BASIN THROUGH MACHINE LEARNING METHODS

Deepak Kumar RAJ✉, Gopikrishnan T.

Department of Civil Engineering, National Institute of Technology Patna, Patna, India

Highlights:

- data integration: This study combines observed and climate model data to analyse climate change in the lower Mahanadi River basin;
- bias correction: Innovative bias correction techniques enhance the accuracy of climate projections by rectifying simulated data;
- effective forecasting: Four machine learning models forecast precipitation and temperature, with Fbprophet and SARIMAX standing out for their performance;
- decadal trends: Decadal projections of precipitation and temperature patterns reveal shifts under different future scenarios;
- visualizing climate shifts: Utilizing ArcGIS for spatial analysis, this study provides intuitive visualizations of projected climate variability, facilitating easy comparisons between historical and future scenarios.

Article History:

- received 20 January 2023
- accepted 27 June 2024

Abstract. This study examined climate change dynamics in the lower Mahanadi River basin by integrating observed and climate model data. Historical precipitation and temperature data (1979–2020) from the India Meteorological Department (IMD) and monthly climate model data from the CORDEX-SMHI-MIROC model via the Earth System Grid Federation (ESGF) are utilized. Four machine learning models (Fbprophet, Holt-Winters, LSTM RNN, and SARIMAX) are applied to forecast precipitation, T_{max}, and T_{min}, and are compared across different representative concentration pathway (RCP 2.6, 4.5, and 8.5) scenarios. Diverse trajectories emerge, highlighting potential shifts in precipitation and temperature dynamics over near, mid, and far-term intervals. Fbprophet and SARIMAX are identified as superior models through performance evaluation metrics (R^2, RMSE, r, P-bias, and NSE). Spatial analysis using ArcGIS and IDW interpolation reveals spatial variations in climate projections, aiding in visualizing future climate trends within the Mahanadi Basin. This study acknowledges limitations such as historical data uncertainties, socio-economic indicators, and unpredictable RCP trajectories, introducing a novel method to integrate machine learning with climate model data for assessing reliability. It also explores anticipated shifts in monthly precipitation and temperature patterns, providing insights into future climate variations.

Keywords: climate model, machine learning, precipitation, temperature, Mahanadi Basin.

✉Corresponding author. E-mail: ***dkraj.iitbhu2018@gmail.com***

1. Introduction

In the present era, there is a heightened awareness and concern regarding climate change, a phenomenon that poses significant challenges and implications for the future. Climate change has the potential to exacerbate and prolong droughts or floods, leading to adverse impacts on various aspects of society and the environment. This heightened concern underscores the urgent need for proactive measures and strategies to mitigate and adapt to the anticipated impacts of climate change. As the planet edges closer to the critical 1.5 °C threshold due to global warming, the risk of more severe climate disasters looms large. This poses increased dangers to both people and nature. We need to act fast to prevent further warming and protect ourselves and our environment (Intergovernmental Panel on Climate Change [IPCC], 2022). It is crucial to anticipate future climatic shifts, especially when considering their effects on river basins. Climate change has long been recognized as a significant factor influencing hydrology and water resources. Understanding these impacts is essential for effective management and adaptation strategies. This recognition highlights the urgent need for proactive measures to address the challenges posed by climate change in water management (Fiseha et al., 2014). Given the sensitivity of regional hydrology to a shifting climate (Saranya & Vinish, 2021), climate change projections assume a critical role in evaluating recent and impending alterations within the hydrological cycle. Such projections often hinge upon climate models and pivotal climatic parameters such as temperature and precipitation.

The evaluation of climate change repercussions on environmental dynamics, meteorological events, and climatic patterns necessitates the utilization of regional climate models (RCMs), propelled by an array of scenarios and grounded in statistical, physical, or dynamical downscaling of model simulations and prognostications from these RCMs (Perkins et al., 2014). These climate studies rely upon the precipitation and temperature projections derived from these climate models. The World Climate Research Program spearheads an intercomparison initiative, fostering collaboration and comparison among researchers' models worldwide. In the South Asia context, the Coordinated Regional Downscaling Experiment (CORDEX) took flight in 2009, fostering a framework for assessing and validating downscaling models. The CORDEX initiative sets forth a series of experiments, yielding climate forecasts that fuel studies on impacts and adaptability. Notably, researchers have forecasted an upward trajectory in the average annual temperature of India (Krishna Kumar et al., 2011).

In the realm of climate prediction, time series machine learning models have emerged as pivotal tools for predicting precipitation and temperature patterns. While an array of time series machine learning methodologies exist, Facebook Prophet (Fbprophet), Holt-Winters, Long Short-Term Memory Recurrent Neural Network (LSTM RNN), and Seasonal AutoRegressive Integrated Moving Average with eXogenous factors (SARIMAX) have emerged as optimal options for grappling with rainfall and temperature data. These models offer distinct and efficient approaches for handling time series data (Jose et al., 2022). Notably, the landscape of weather forecasting and research originally evolved around statistical methodologies. For instance, the seasonal ARIMA model was harnessed by (Graham et al., 2017) for forecasting and modelling rainfall (Dhamodharavadhani & Rathipriya, 2019). Holt Winter's smoothing method is the most accurate approach for predicting monthly rainfall across regions. In a similar vein, Khan et al. (2020) advocated for the efficacy of the LSTM model in predicting monthly temperature and precipitation. Affirmative outcomes in forecasting monthly peak seasonal precipitation and temperature data in the Himalayan region are attributed to the Fbprophet model (Haq, 2022).

This study has a dual objective: first, to rectify systematic biases present in precipitation and temperature projections derived from climate models. This involves utilizing the CMhyd tool to extract data from regional climate models and subjecting it to bias correction. Second, the research aims to evaluate and compare the performance of machine learning models, including Fbprophet, Holt Winter's, LSTM RNN, and SARIMAX, in accurately reproducing historical climate data (Chaturvedi et al., 2022). This entails assessing the effectiveness of machine learning models in replicating historical climate patterns and identifying the most reliable model for future projections. Additionally, the research compares projected historical climate data with future climate scenarios projected under different Representative Concentration Pathways (RCPs) to discern potential differences and improve understanding of future climate trends. Our research also extends to investigating anticipated shifts in monthly precipitation and temperature patterns, providing valuable insights into the potential variations shaping the future climate of the Lower Mahanadi Basin.

2. Study area

India has 12 significant river basins and the basin of the Mahanadi River basin ranks 8th in India having a total watershed area of nearly 1,39,681.5 km^2. This accounts for around 4.30 percent of India's entire geographical area. The Mahanadi Basin is located between latitudes 19°8′ and 23°32′ North and longitudes 80°28′ to 86°43′ East (Figure 1). The Mahanadi Basin is surrounded by the central Indian mountains which are in the North direction. The basin is surrounded by the Eastern Ghats of India in the both South direction and the East direction. The Maikalaa mountain range is in the West direction. The length of the basin is approximately 586 km whereas the width of the basin is approximately 400 km which looks Mahanadi Basin is nearly round. The basin is divided into three parts, the lower Mahanadi Basin which is situated in the coastal

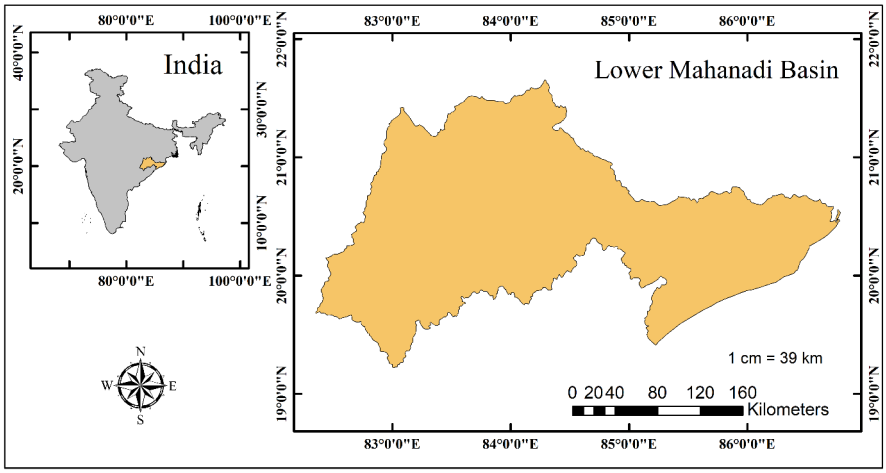

Figure 1. Map of study area showing Lower Mahanadi River basin (the map is generated in ArcGIS software by the authors)

part of India the middle Mahanadi Basin, and then the upper Mahanadi Basin (Dadhwal et al., 2014; Mujumdar & Ghosh, 2008).

The geography of the Mahanadi Basin is diverse, the coastal regions have the lowest elevation whereas the northern highlands have the highest elevation. The basin has been divided into eleven elevation zones using the SRTM DEM (Shuttle Radar Topography Mission Digital Elevation Model). The Mahanadi Basin experiences the cold, hot, southwest monsoon, and post-monsoon seasons. Winters are nice since the weather is bright and the winds are frequently mild, blowing from the north or northeast. During the monsoon season (June to October) more than 90% of the annual precipitation occurs. Precipitation comes in bursts of varying lengths and intensities, rather than as a constant stream the warmest months in this region are April and May. The average maximum temperatures are likely to be in the range of 39 °C to 40 °C.

The Seonath, Arpa, Kurung, and Sakri Rivers drain the upper subbasin of the Mahanadi River. The Mand, Bhedan, IB, and Jonk Rivers constitute the Mahanadi middle subbasin, and the Ong, Tel, Hati, and Daya Rivers drain into the Mahanadi lower subbasin. The coastal and southern regions of the basin are covered by the Mahanadi lower subbasin (Kannan & Ghosh, 2011). The upper Mahanadi sub-basin is 21.34 percent of the entire geographic region of the Mahanadi Basin which accounts for 29,796.64 km^2. The middle Mahanadi subbasin covers 37.16 percent of the Mahanadi Basin's entire geographical area which accounts for 51,895.90 km^2. The Size Range of the watershed of the upper Mahanadi subbasin is approximately 314.34 to 907.60 km^2 and has 48 watersheds and the size range of the watershed of the middle Mahanadi subbasin is approximately 301.22 to 902.46 km^2 and has 88 watersheds. The climate is tropical with a hot and moist monsoonal climate. Since Mahanadi depends primarily on rainfall, there are significant seasonal variations in the water availability.

Because of the watershed's proximity to the Bay of Bengal, its weather and climatology are highly impacted which is where the majority of weather systems originate. The IMD (India Meteorological Department), CWC (Central Water Commission), and Automatic Weather Stations of ISRO are the 3 primary organizations in India that record meteorological features. The basin is home to thirteen CWC (Central Water Commission) meteorological stations. At these locations, rainfall, temperature, pan evaporation, moisture content, wind velocity, sunlight, and other climatic indicators were measured according to indiawris government website, of the 2014 basin report.

3. Data set

The study's data foundation is rooted in two distinct datasets: observed data and climate model data. The former, acquired from the India Meteorological Department (IMD), comprises precipitation and temperature records sourced from a network of stations across the expansive Mahanadi River basin. IMD's diligent collection efforts have yielded comprehensive daily historical time series data, encapsulating area-averaged precipitation and temperature dynamics (Pattanaik & Das, 2015).

Complementing this observed dataset, the study harnesses monthly climate model data procured from the Earth System Grid Federation (ESGF), a reputable repository endorsed by the Intergovernmental Panel on Climate Change (IPCC). Specifically, the CORDEX-SMHI-MIROC-5 Regional Climate Model output serves as the focal point of the investigation, accessible through the Climate4impact platform (IS-ENES3 C4I-Search, 2022). Facilitated by European initiatives (IS-ENES, IS-ENES2, CLIPC), Climate4impact offers a conduit for the practical utilization of climate research data, fortified by integration with ESGF and robust authentication mechanisms (Déandreis et al., 2014).

The choice of the CORDEX-SMHI-MIROC-5 model is underpinned by its alignment with the Coordinated Regional Climate Downscaling Experiment (CORDEX) mission, exemplifying collaborative global efforts in regional climate downscaling. This selection finds validation in Jain et al.'s work (2019), wherein the model's adeptness in capturing Indian summer monsoon precipitation variability is underscored. Encompassing historical data from 1979 to 2010 and future scenarios projected under representative concentration pathways (RCP 2.6, RCP 4.5, and RCP 8.5) from 2005 to 2050, this model substantiates the study's exploration of climatic dynamics in the lower Mahanadi River basin (Jain et al., 2019).

In the context of hydrologic system forecasting, watershed models often grapple with biases arising from parameter variations and regional averaging in temperature and precipitation simulations. Overcoming these challenges, the study introduces bias correction techniques, rectifying simulated climate data through step adjustments to align with observed records (Teutschbein & Seibert, 2012). At the heart of this correction process lies the CMhyd tool, adept at extracting and rectifying data from global and regional climate models. Integral to bias correction are transformation algorithms, pivotal in reshaping climate model outputs. Parametrizing bias correction hinges on discerning biases by comparing observed and simulated climate data (Salvi et al., 2017). Amidst this intricate interplay, harmonizing these elements lays the foundation for understanding the hydrological ramifications of future climate change.

4. Methodology

In this climate simulation, bias-corrected observed climatic data from the center stage were used as input for the time series machine learning algorithm. Averting the direct use of RCM output, which carries systematic bias, is advised. Rectification of biases in precipitation and temperature projections, stemming from the indicated GCM and RCM pairings, is crucial (IPCC, 2022). Leveraging the CMhyd tool, data from regional climate models is extracted and subjected to bias correction, a process detailed in the CMhyd user manual (Rathjens et al., 2016). This methodology

ensures a more reliable foundation for time series machine learning, enhancing the accuracy of climate simulations (Figure 2).

The process begins with Data Input, which incorporates historical climate data from the Indian Meteorological Department (IMD), simulated historical climate data (CORDEX-SMHI-MIROC-5), and simulated future climate data from the CORDEX-SMHI-MIROC-5 model, under three RCP scenarios (2.6, 4.5, and 8.5). Subsequently, both sets of data undergo bias Correction, utilizing an algorithm to rectify any systematic disparities between simulated and observed data.

The bias-corrected simulated historical climate data are then used to project the historical climate data using machine learning models. This step essentially attempts to reproduce the observed historical climate using the model's capabilities. Following the Projection of Historical Data, the machine learning models undergo a Performance Evaluation to assess their effectiveness in reproducing historical climate data. This evaluation aids in identifying the most reliable model for making future projections.

In the comparison stage, the projected historical climate data from the best machine learning model are compared with the RCP's future climate scenarios. This comparison helps to identify any potential differences between the projected future climate based on the RCP scenarios and the actual historical climate as understood through machine learning models.

The outputs consist of visualizations through graph plots, which offer a quick comparison of trends in projected historical climate data and RCP future scenarios. Additionally, spatial analysis involves geographical representations illustrating how climate change is expected to vary across different regions.

4.1. Description of forecasting models

4.1.1. FBProphet model

FBProphet, developed by Facebook, stands as a prominent tool in time series analysis. This forecasting approach employs an additive algorithm, adept at capturing nonlinear

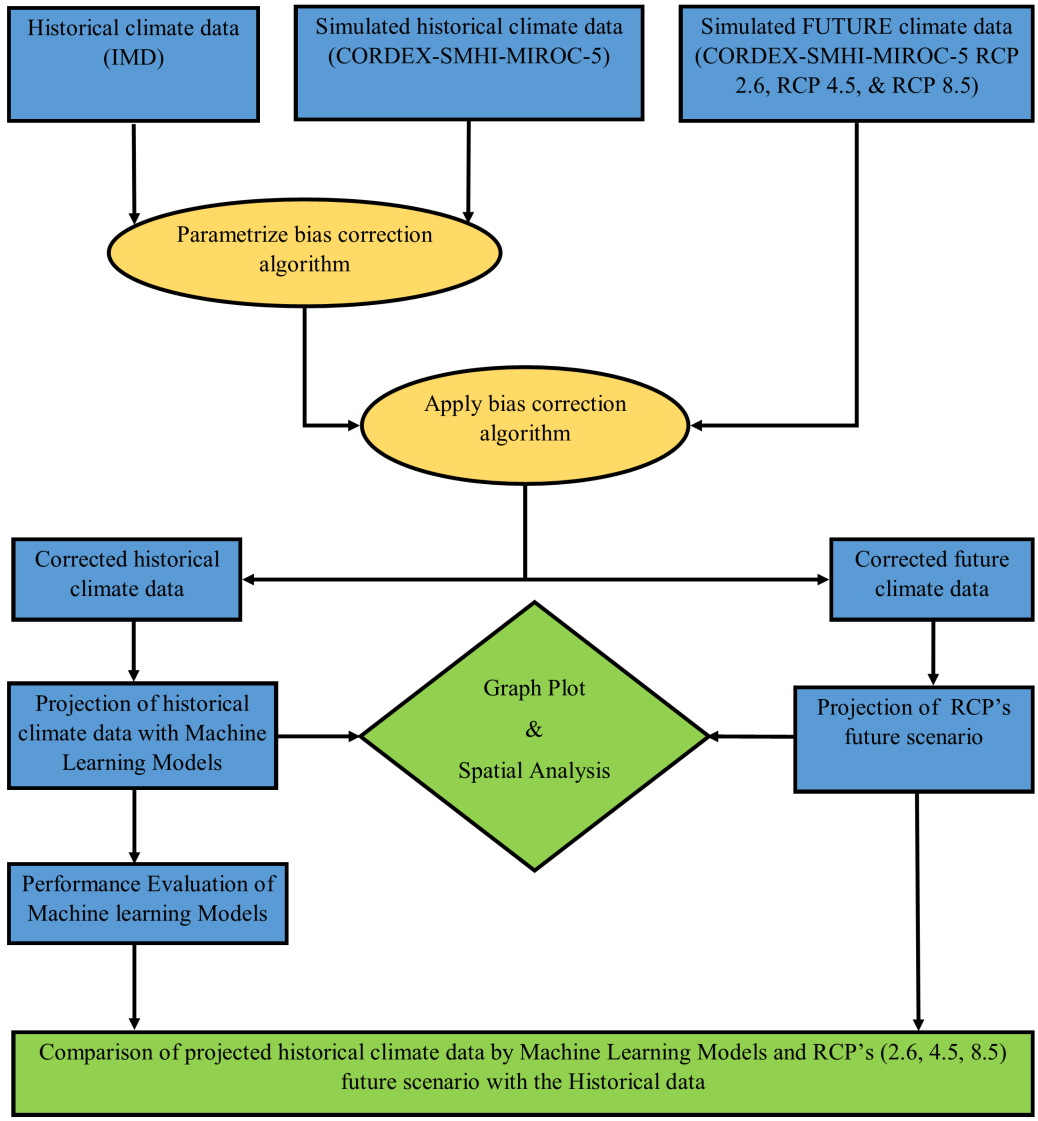

Figure 2. Modified workflow diagram for the bias correction and projection framework within the Climate Model Data for Hydrologic Modelling (CMhyd) (adapted from Rathjens et al., 2016)

trends with annual seasonality across daily and monthly intervals. Notably, FBProphet accommodates the influence of holiday patterns, rendering it robust for seasonal time series and historical data encompassing multiple seasons (Chaturvedi et al., 2022) and available as open-source software in both R and Python (Alam et al., 2021)

4.1.2. Holt Winter model

The Holt-Winters technique is a common time series forecasting methodology that incorporates trend and seasonality. The Holt-Winter methodology may be implemented to time-series data to deal with seasonal variations and trends. Winters' exponential smoothing approach enhances Holt's method by making it easier to accommodate a seasonal component. Because it is created based on both single and double exponential smoothing, Winter's exponential smoothing is often referred to as triple exponential smoothing. Winter's methodology requires a level, trend, and seasonal component in the time-series data (Almazrouee et al., 2020).

4.1.3. LSTM RNN model

Long short-term Memory (LSTM), an architecture rooted in artificial recurrent neural networks (RNNs), constitutes a powerful deep learning paradigm. Comprising LSTM units, an LSTM network's neurons assume the form of memory cells, setting it apart from conventional RNNs (Ishida et al., 2021) (Chaturvedi et al., 2022). LSTM is a type of neural network that links past data to current neurons. Each neuron has three gates: an input gate, a forget gate, and an output gate. The tanh layer, sigmoid layer, and pointwise multiplier operation are also included (Selvin et al., 2017; Tsai et al., 2018). The following are the different gates and their functions.

1. Input gate: The input gate determines which new cell state information should be remembered.
2. Forget gate: The forget gate specifies which information from each cell will be discarded.
3. Output gate: This gate is the LSTM's output.
4. Cell State: This program runs throughout the connection and adds and deletes data using gates. The sigmoid layer produces values ranging from 0 to 1, signifying how much of each element should be allowed to flow through.
5. A new set is obtained by the tanh layer, which is then stored in the state.

4.1.4. SARIMA eXogenous model

SARIMAX is a mathematical prediction model that integrates exogenous components and accounts for time series dependency over seasons. The SARIMAX model is a version of the SARIMA model that integrates exogenous (outside of the model) factors to increase forecasting ability. With a differentiating operator, the model consists of two basic parts: an autoregressive part and a moving average part (Vagropoulos et al., 2016; McHugh et al., 2019).

4.2. Description of bias correction tool

4.2.1. CMhyd tool

The CMhyd tool is a powerful software solution designed to facilitate the preparation of simulated climate change data for hydrologic impact studies. Developed by a team of experts, including Hendrik Rathjens, Katrin Bieger, Raghavan Srinivasan, Indrajeet Chaubey, and Jeffrey G. Arnold, CMhyd addresses a crucial challenge in climate modelling – biases in simulated climate data that hinder accurate hydrological simulations. CMhyd enables users to extract and bias-correct data obtained from global and regional climate models, enhancing their reliability for hydrological modelling applications. CMhyd stands for climate model data for hydrologic modelling.

CMhyd, originating from the Soil and Water Assessment Tool (SWAT), serves as a vital programming tool designed to bridge climate simulations and hydrological models. Its primary role revolves around furnishing climate simulation data to determine optimal gauge placement within hydrological models (Rathjens et al., 2016). By harnessing climate model data tailored for specific gauge positions, CMhyd undertakes the essential task of data acquisition and subsequent bias correction. Remarkably, the bias correction methodology, along with its experimental parameters, exhibits applicability not only to historical data but also extends its utility to forecasted climate scenarios. This forward-looking adaptability underscores the tool's capacity to harmonize the same bias correction technique for rectifying future climate data (Teutschbein & Seibert, 2012). Presently, the prevailing and widely embraced approach for bias correction is linear scaling, a technique recurrently employed in diverse studies (Ines & Hansen, 2006).

In pursuit of refining climate model outputs, bias correction procedures harness a transformative algorithm. This pivotal approach rests upon the fundamental tenet of pinpointing disparities between observed and projected historical meteorological data, thereby rectifying the synthesized historical climate data. Developed using Python 2.7, CMhyd exemplifies a potent solution in this domain, employing a suite of vital Python packages including NetCDF41, NumPy, SciPy, and the PyQt42 application framework. This amalgamation of tools empowers CMhyd to execute its role as a versatile and effective instrument for enhancing climate modelling precision and facilitating seamless integration into hydrological analyses.

CMhyd's core objective revolves around delivering tailored simulated climate data for precise gauge locations, facilitating subsequent extraction and bias correction of climate model data at individual gauge stations. This correction process, which is crucial for enhancing climate model outputs, employs various bias correction methods driven by a transformation algorithm. CMhyd efficiently identifies climate model grid cells aligned with gauge stations, leveraging netCDF file metadata. Through this process, temperature and precipitation data are seamlessly converted into degrees Celsius and

millimeters, respectively (Yeboah et al., 2022). CMhyd boasts a repertoire of eight distinct bias correction techniques, with the current study highlighting the implementation of linear scaling methods as a pivotal approach to enhance accuracy (Das et al., 2022). This amalgamation of functionalities positions CMhyd as a versatile and indispensable tool for optimizing climate data integration within hydrological assessments.

5. Results

5.1. Performance evaluation of machine learning models for precipitation, T_{max}, and T_{min} forecasting in the Mahanadi Basin

In this research, the forecasting of precipitation, T_{max}, and T_{min} was conducted using Python with four distinct machine learning models, namely Fbprophet, Holt-Winters, LSTM RNN, and SARIMAX. Historical monthly data spanning from 1979 to 2020 for the lower Mahanadi Basin has been employed, while future data forecasting was based on the period from 1979 to 2010. Model validation was performed using historical monthly data up to 2020. The evaluation of model performance encompassed a comprehensive set of statistical performance indicators, including the coefficient of determination (R^2), root mean square error (RMSE), coefficient of correlation (r), percentage bias (P-bias), and Nash-Sutcliffe efficiency (NSE) (Table 1). This robust methodology ensures rigorous and accurate evaluation of the predictive capabilities of the chosen machine learning models.

Table 1. Performance evaluation of different models using statistical metrics

	Parameter	R^2	RMSE	r	P-bias	NSE
Fbprophet	Precipitation	0.763	0.957	0.873	0.373	0.843
	T_{max}	0.8883	0.0029	0.9424	–0.1197	0.5528
	T_{min}	0.947	0.021	0.973	–0.040	0.959
Holt-Winters	Precipitation	0.746	1.818	0.864	0.339	0.818
	T_{max}	0.8919	0.0753	0.9443	–0.1011	0.7459
	T_{min}	0.953	0.003	0.976	–0.035	0.974
LSTM RNN	Precipitation	0.297	2.138	0.545	0.397	0.464
	T_{max}	0.8393	0.0325	0.9161	–0.0901	0.7476
	T_{min}	0.870	0.042	0.932	–0.038	0.947
SARIMAX	Precipitation	0.757	0.965	0.870	0.371	0.839
	T_{max}	0.8932	0.025916	0.9450	–0.1122	0.6804
	T_{min}	0.953	0.024	0.976	–0.040	0.972

In the evaluation of different models for predicting precipitation, T_{max} (maximum temperature), and T_{min} (minimum temperature), various performance metrics were considered. Fbprophet and SARIMAX consistently exhibited strong performance across the parameters, boasting higher R^2 and NSE values, indicative of superior predictive capability and fit. Moreover, both models demonstrated lower P-bias values, reflecting reduced bias in predictions. While LSTM RNN demonstrated competitive results, its NSE values were comparatively lower. Overall, the combination of Fbprophet and SARIMAX emerged as favourable choices for all three parameters due to their robust performance across multiple evaluation metrics.

5.2. Decadal changes in precipitation and temperature patterns: addressing biases and unveiling temporal trends

We addressed biases within the RCP (2.6, 4.5, and 8.5) scenarios using a precise linear scaling approach. Subsequently, we categorized the corrected data into near-term (2021–2030), mid-term (2031–2040), and far-term (2041–2050) intervals, as outlined in Table 2. Our approach meticulously rectified biases, ensuring robustness. Linear scaling enhanced data alignment with historical patterns, bolstering projection reliability. Categorization into temporal segments offers comprehensive insights into evolving trends over decades.

We present changes in precipitation (%) and dynamic temperature interplay against historical benchmarks. These data are encapsulated in the concise table "Decadal Changes of Projected Precipitation, T_{max}, and T_{min} from Four Different Machine Learning Models and Three RCP Scenarios in the Lower Mahanadi Basin." This framework showcases our study's holistic approach and deepens our understanding of the region's changing climate.

5.2.1. The near-term (2021–2030) Fbprophet, Holt Winter, LSTM RNN, and SARIMAX models and under the three RCP (2.6, 4.5, and 8.5) scenario

In the decade ahead (2021–2030), advanced models shed light on potential shifts in the climate of the Mahanadi Basin. Predictions of annual average precipitation and temperature changes, using various methods and scenarios, yield intriguing findings. Holt Winter's model (Figure 6) foresees a substantial 10.50% surge in annual average precipitation, suggesting heightened rainfall trends. However, Fbprophet, LSTM RNN, and SARIMAX models (Figure 6) diverge, indicating slight to moderate declines of 3.59%, 1.00%, and 4.01% respectively. RCP scenarios unravel diverse trajectories: RCP 2.6 suggests a marginal 0.19% rise, RCP 4.5 projects a more notable 6.97% increase, while RCP 8.5 paints a contrasting picture with an 8.94% decrease.

Shifting the focus to temperature, forecasted patterns reveal captivating dynamics. Maximum temperature projections (Figure 3a) signal annual average increments,

Table 2. Decadal changes of projected precipitation, $T_{max,}$ and T_{min} from four different machine learning models and three RCP scenarios in the lower Mahanadi Basin

	Models and RCPs	Fbprophet	Holt winter's	LSTM RNN	SARIMAX	RCP 2.6	RCP 4.5	RCP 8.5
2021–2030	Precipitation	–3.59%	10.50%	–1.00%	–4.01%	0.19%	6.97%	–8.94%
	T_{max}	2.13	0.56	–0.37	0.79	0.45	0.70	0.92
	T_{min}	2.49	1.22	–0.45	1.54	0.35	0.63	0.43
2031–2040	Precipitation	–4.78%	14.18%	–1.02%	–5.23%	–8.62%	8.16%	3.28%
	T_{max}	2.89	1.00	–0.36	1.02	0.74	1.27	0.88
	T_{min}	3.37	1.52	–0.43	1.96	0.57	1.04	0.65
2041–2050	Precipitation	–5.91%	16.10%	–1.01%	–6.45%	9.29%	–7.37%	4.26%
	T_{max}	3.64	1.43	–0.37	1.26	0.49	1.84	1.14
	T_{min}	4.24	1.83	–0.41	2.38	0.64	1.31	1.16

with Fbprophet predicting a 2.13 °C rise, Holt Winter predicting a 0.56 °C increase, and SARIMAX predicting a 0.79 °C elevation. Intriguingly, LSTM RNN takes a different route, hinting at a 0.37 °C reduction. Similarly, for minimum temperature, Fbprophet, Holt Winter, and SARIMAX models predict gains of 2.49 °C, 1.22 °C, and 1.54 °C respectively, while the LSTM RNN suggests a decrease of 0.45 °C.

Noteworthy seasonal patterns emerge, with peak precipitation observed in July and August (380 mm to 450 mm), while minimal levels occur in December and January (15 mm to 20 mm). Temperature extremes manifest in May (44 °C) and December/January (13 °C), contributing to a rich portrayal of upcoming climatic intricacies. These multifaceted predictions, illustrated in Figures 6 and 3a, provide valuable insights into the potential climatic landscape ahead.

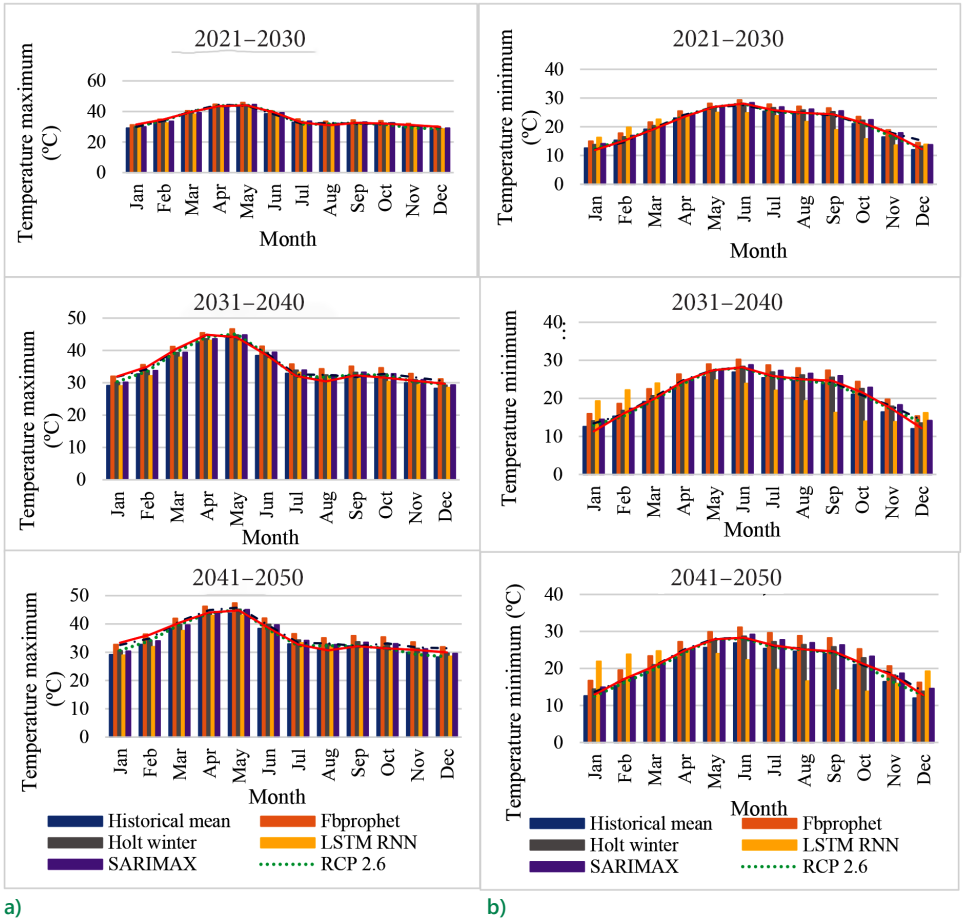

Figure 3. a) The graph shows the monthly average temperature maximum of observed data and projected data in near (2021–2030), mid (2031–2040) and far (2041–2050) term from four different time series machine learning models and three RCP scenarios (RCP 2.6, RCP 4.5 and RCP 8.5) in the lower Mahanadi Basin; b) The graph shows the monthly average temperature minimum of observed data and projected data in near (2021–2030), mid (2031–2040) and far (2041–2050) term from four different time series machine learning models and three RCP scenarios (RCP 2.6, RCP 4.5 and RCP 8.5) in the lower Mahanadi Basin

5.2.2. The mid-term (2031–2040) from Fbprophet, Holt Winter's, LSTM RNN, SARIMAX model and under the three RCPs' (2.6, 4.5, and 8.5) scenario

Starting with precipitation, when compared to historical data, Holt Winter's model points to a substantial 14.18% increase in average annual rainfall. In contrast, Fbprophet, LSTM RNN, and SARIMAX models present different results, suggesting percentage decreases of 4.78%, 1.02%, and 5.23%, respectively. Interestingly, RCP 4.5 and RCP 8.5 show an anticipated increase in annual average precipitation, with percentages of 8.16% and 3.28% respectively. However, RCP 2.6 predicts a decrease of 8.62%. These trends align with a consistent rhythm observed in both RCP scenarios and machine learning models, showing peak rainfall in July and August (ranging from 385 mm to 465 mm) and a subdued period in December and January with minimal rainfall (15 mm to 20 mm) (Figure 6).

Concerning temperature, the models provide valuable insights. For maximum temperatures, the Fbprophet, Holt Winter, and SARIMAX models converge, predicting annual

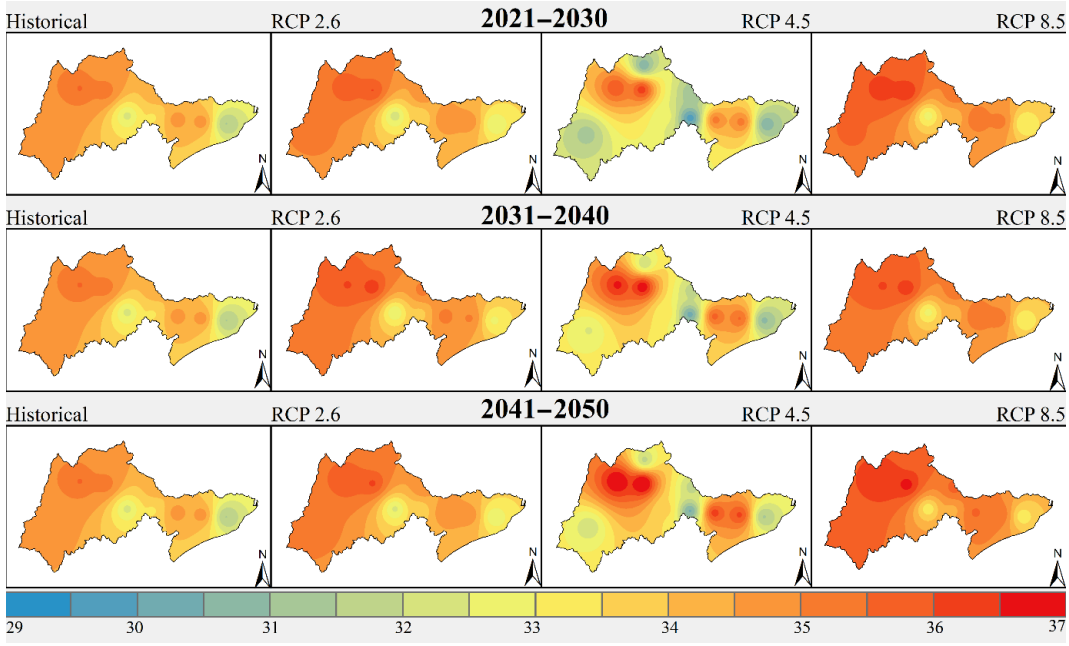

Figure 4. Projected variability in annual maximum temperatures across three time periods: near (2021–2030), mid (2031–2040), and far (2041–2050). These projections are compared to the historical period (1979–2010) and evaluated under three RCP scenarios (RCP 2.6, RCP 4.5, and RCP 8.5)

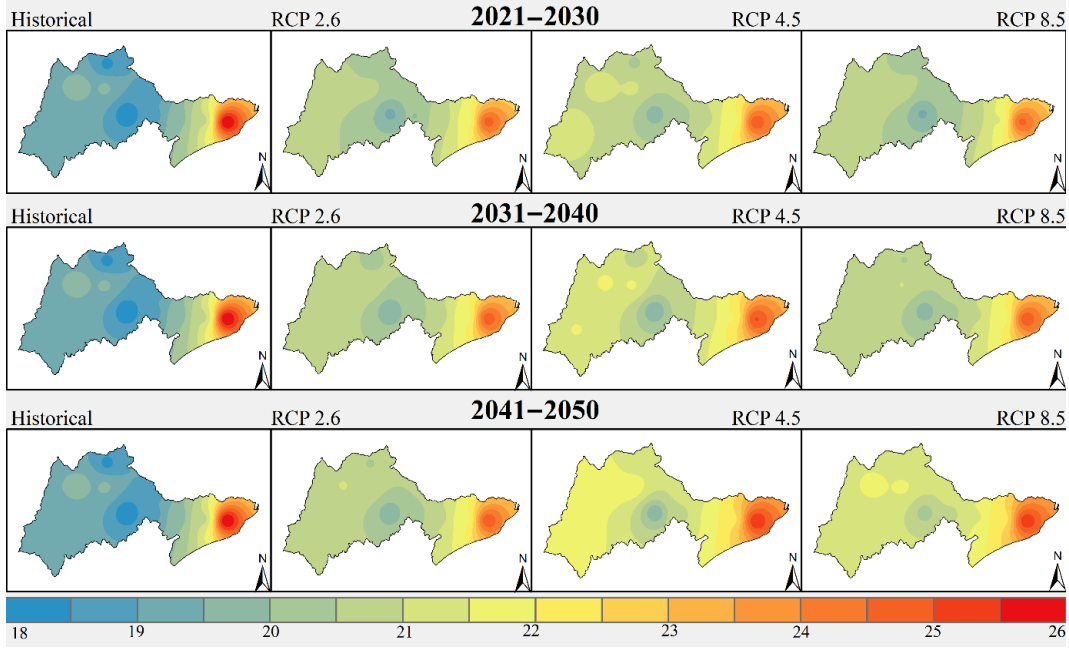

Figure 5. Projected variability in annual minimum temperatures across three time periods: near (2021–2030), mid (2031–2040), and far (2041–2050). These projections are compared to the historical period (1979–2010) and evaluated under three RCP scenarios (RCP 2.6, RCP 4.5, and RCP 8.5)

average increments. Fbprophet forecasts a rise of 2.89 °C, Holt Winter predicts a rise of 1.00 °C, and SARIMAX suggests a rise of 1.02 °C. Interestingly, the LSTM RNN predicts a different scenario, hinting at a decrease of 0.36 °C in the annual average maximum temperature.

Similar trends emerge for minimum temperatures. The Fbprophet, Holt Winter, and SARIMAX models predict annual average increases. Fbprophet indicates a substantial rise of 3.37 °C, Holt Winter's 1.52 °C, and SARIMAX 1.96 °C. In contrast, LSTM RNN introduces a unique perspective, suggesting a decrease of 0.43 °C. This analysis revealed consistent temperature patterns across both RCP scenarios and machine learning models. The coldest months, December and January, experience temperatures dropping to ~14 °C minimum, while the warmest readings are in May, reaching ~28 °C minimum (Figure 3b).

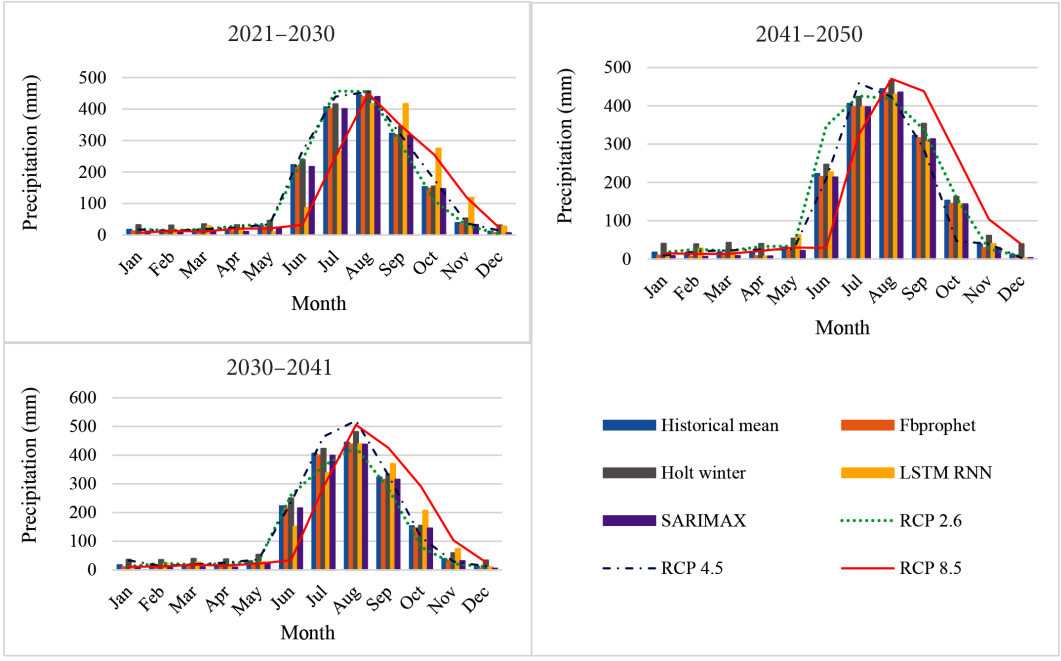

Figure 6. The graph shows the monthly average precipitation of historical data and projected data in near (2021–2030), mid (2031–2040) and far (2041–2050) term from four different time series machine learning models and three RCP scenarios (RCP 2.6, RCP 4.5 and RCP 8.5) in the lower Mahanadi Basin

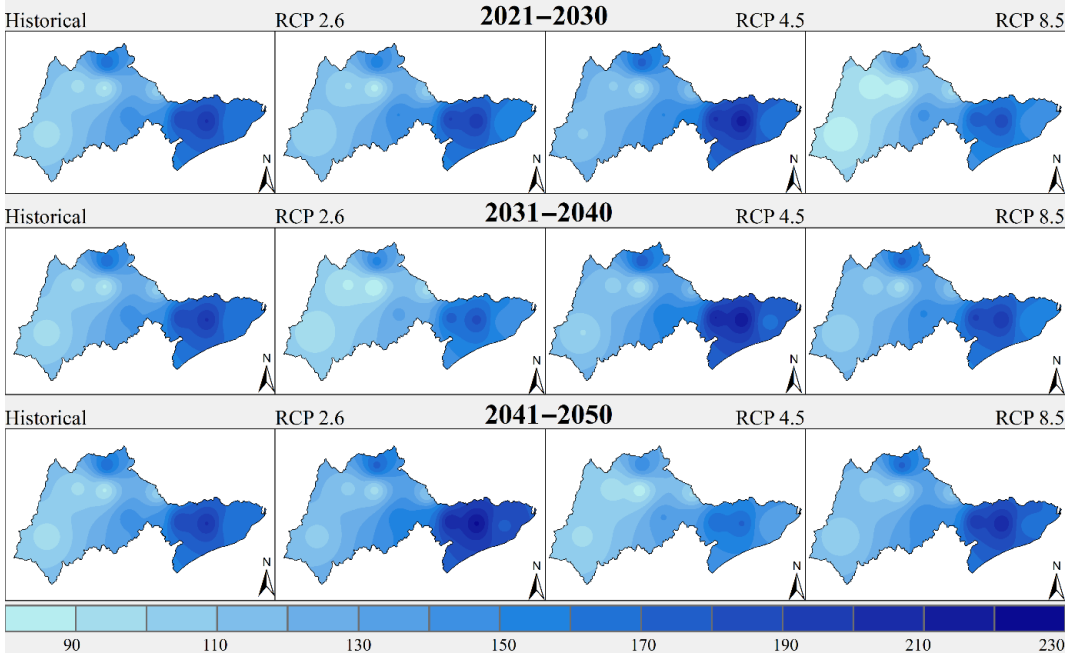

Figure 7. Projected variability in precipitation for the near (2021–2030), mid (2031–2040), and far (2041–2050) terms compared to the historical period (1979–2010), across RCP scenarios (RCP 2.6, RCP 4.5, and RCP 8.5)

In conclusion, this detailed exploration of mid-term climate projections, visualized in Figures 6 and 3a-b, deepens our understanding of potential climate dynamics. This study highlights the intricate relationships between various models and scenarios, aiding our comprehension of future climatic shifts.

5.2.3. The far-term (2041–2050) Fbprophet, Holt Winter, LSTM RNN, and SARIMAX models and under the three RCP (2.6, 4.5, and 8.5) scenario

Starting with precipitation, a comparison with historical data yields intriguing results. Holt Winter's model forecasts a substantial 16.10% rise in annual average rainfall during this far-reaching period. Conversely, Fbprophet, LSTM RNN, and SARIMAX models portray a different outlook, indicating percentage decreases of 5.91%, 16.10%, and 6.45% respectively. Intriguingly, RCP 2.6 and RCP 8.5 envision an uptick in annual average precipitation, with percentages of 8.16% and 3.28% respectively. However, RCP 4.5 presents an alternative perspective, suggesting a decrease of 7.37%. Echoing a consistent rhythm across both RCP scenarios and machine learning models, we witness peak precipitation in July and August (ranging from 403 mm to 440 mm), while December and January usher in a period of minimal rainfall (10 mm to 20 mm) (Figure 6).

Shifting the focus to temperature dynamics, these models offer crucial insights. For maximum temperatures, a convergence of predictions is observed. Fbprophet, Holt Winter, and SARIMAX models anticipate annual average increments. Fbprophet envisions a rise of 3.64 °C, Holt Winter suggests 1.43 °C, and SARIMAX points to 1.26 °C. Notably, the LSTM RNN deviates from this trend, indicating a decrease of 0.37 °C in the annual average maximum temperature.

Likewise, a common thread emerges in minimum temperature projections. The Fbprophet, Holt Winter, and SARIMAX models forecast annual average increases. Fbprophet projects a substantial rise of 4.24 °C, Holt Winter at 1.83 °C, and SARIMAX at 2.38 °C. Interestingly, the LSTM RNN introduces an alternate view, suggesting a decrease of 0.41 °C.

In parallel to the broader context, a consistent rhythm persists in temperature patterns across both RCP scenarios and machine learning models. The coolest months, December and January, experience temperatures reaching ~15 °C minimum, while May boasts the highest readings at ~28 °C minimum (Figure 3b). In summation, this in-depth exploration of far-term climate predictions, as elucidated in Figures 6 and 3a, 3b, augments our understanding of potential climatic trajectories. It underscores the intricate connections between diverse models and scenarios, deepening our comprehension of impending climate dynamics.

5.3. Visualizing future climate trends in the Mahanadi Basin through spatial analysis

ArcGIS and the inverse distance weighting (IDW) interpolation technique were utilized. To perform IDW interpolation, a network of strategically selected station points was established across the Mahanadi Basin. These points, thoughtfully positioned for comprehensive coverage, facilitated accurate and detailed spatial representations of the climate variables. This approach enhances the precision and reliability of our spatial analyses. This study visually depicts projected climate changes in the Mahanadi Basin. Historical and three RCP scenarios (RCP 2.6, RCP 4.5, RCP 8.5) are color-coded, highlighting anticipated variability in annual maximum and minimum temperatures, as well as precipitation across near (2021–2030), mid (2031–2040), and far (2041–2050) timeframes. This spatial representation facilitates easy comparison with the historical period (1979–2010), aiding in the assessment of RCP impacts. The map serves as a comprehensive tool for intuitively grasping the geographic extent and spatial nuances of climate shifts, offering valuable insights for researchers and decision-makers alike, and aiding in the understanding of the evolving climatic dynamics within the Mahanadi Basin.

Figure 4 illustrates projected variability in annual maximum temperatures across three time periods: near (2021–2030), mid (2031–2040), and far (2041–2050). These projections are compared to the historical period (1979–2010) and evaluated under three RCP scenarios (RCP 2.6, RCP 4.5, and RCP 8.5).

6. Discussion

When we compared historical data using four different time-based machine learning models, the projected precipitation in the lower Mahanadi Basin suggested that the expected climate changes might not lead to a significant alteration in the total amount of precipitation received in the study area. However, the distribution of this precipitation across different seasons is likely to undergo significant changes. The chosen climate scenario (RCP) and the specific time under consideration play crucial roles in determining the annual precipitation trends, which exhibit notable variability along the coastal zone in the eastern region.

All considered climate scenarios indicate an increase in annual precipitation across all examined periods (Figure 7). In the case of the RCP 2.6 scenario (Figure 7), the projected precipitation pattern resembles the historical trends during the near-term period of 2021–2030. In a considerable portion of the western region, except near the coast, there is a possibility of reduced precipitation compared to historical levels. This pattern is also observed in certain central and northern areas. These anticipated changes are characterized across three distinct time phases (the 2030s, 2040s, and 2050s), aligning with the approach taken by (Mavume et al., 2021).

Under the RCP 4.5 scenario (Figure 7), projections indicate increased precipitation near the coastal regions of the eastern area for both the near-term (2021–2030) and far-term (2031–2040) periods, in contrast to historical values and RCP 2.6 predictions. However, a slight decrease in coastal precipitation is expected during the far-term period (2041–2050). The RCP 8.5 and RCP 2.6 scenarios demonstrate similar precipitation patterns, with a marginal decline observed across all three-time phases. By the mid-century, a discernibly

uneven distribution of precipitation across the region becomes evident compared to historical conditions.

Anticipated changes over three time periods (2021–2030, 2031–2040, and 2041–2050) reveal that the highest annual temperatures will exceed historical records. While the coastal region of the lower Mahanadi Basin will experience relatively minor fluctuations, more significant temperature variations are expected in the interior and western areas. This observation aligns with findings by (Vijayakumar et al., 2021) and a report on the Mahanadi Basin published by the Water Resources Department of India.

Under the RCP 2.6 scenario (Figure 4), there is a consistent pattern of temperature increase across almost all three analysis periods. The western segment of the lower Mahanadi Basin shows elevated temperatures in comparison to the historical norm. In the lower basin, following the RCP 2.6 scenario, temperatures are projected to rise by approximately 0.45 °C in the near-term, 0.75 °C in the mid-term, and 0.50 °C in the far term (2021–2030, 2031–2040, and 2041–2050, respectively).

In the case of the RCP 4.5 scenario, temperature changes are relatively lower in certain parts of the lower Mahanadi Basin when compared to the RCP 2.6 scenario (Figure 4). The lower basin is expected to experience temperature increases of about 0.70 °C, 1.27°C, and 1.84 °C during the three time periods (2021–2030, 2031–2040, and 2041–2050, respectively).

Under the RCP 8.5 scenario, more substantial temperature changes are anticipated across the entire basin. The lower Mahanadi Basin is projected to encounter temperature rises of approximately 0.92 °C, 0.88 °C, and 1.14 °C over the three time periods (2021–2030, 2031–2040, and 2041–2050, respectively).

Projected changes over the next three periods (2021–2030, 2031–2040, and 2041–2050) indicate that the minimum annual temperatures will be higher than historical records. While the coastal region of the lower Mahanadi Basin will experience relatively stable temperatures, more pronounced temperature shifts are expected in the interior and western areas. This finding aligns with (Vijayakumar et al., 2021) and the Mahanadi Basin report published by the Indian Ministry of Water Resources Department.

Examining the RCP 2.6 scenario (Figure 5) reveals a consistent pattern of increasing minimum temperatures across almost all three time periods. The western part of the lower Mahanadi Basin shows elevated temperatures compared to the historical baseline. Under the RCP 2.6 scenario, the lower basin is projected to experience temperature increases of approximately 0.45 °C in the near term, 0.75 °C in the mid-term, and 0.50 °C in the far term (2021–2030, 2031–2040, and 2041–2050, respectively).

The RCP 4.5 scenario presents a comparatively lower temperature change in certain parts of the lower Mahanadi Basin when compared to RCP 2.6 (Figure 5). The lower basin is projected to see temperature increases of approximately 0.35 °C, 0.57 °C, and 0.64 °C during the three time periods (2021–2030, 2031–2040, and 2041–2050, respectively). On the other hand, the RCP 8.5 scenario indicates larger temperature fluctuations compared to RCP 2.6 and historical trends (Figure 5), with the lower Mahanadi Basin experiencing temperature increases of approximately 0.63 °C, 1.04 °C, and 1.31 °C over the same three time periods.

Considering the broader context, according to (Fadnavis et al., 2020) the average surface air temperature variation in India's CORDEX model for the mid-term phase (2040–2069) relative to historical data (1976–2005) is anticipated to range between 1.39 °C to 2.70 °C. In the long-term phase (2070–2099), relative to the same historical data, the anticipated temperature variation is projected to be between 1.33 °C to 4.44 °C under scenarios of global warming caused by greenhouse gases.

The outcomes of this study unveil an uneven distribution of precipitation alongside an evident increase in both maximum and minimum temperatures across the region. As a result, it is conceivable that heatwaves could become more frequent, intense, and expansive, spanning a larger geographical extent from the mid-to late-21st century, in line with insights by (Rohini et al., 2019) and (Fadnavis et al., 2020).

In the context of the lower Mahanadi Basin, our findings support the notion of heightened precipitation levels during July and August, a trend that aligns with the observations made by (Swain, 2016). Furthermore, spanning the entirety of the lower Mahanadi Basin, it is anticipated that both maximum and minimum temperatures will experience an elevation during May and June, while reaching their lowest points in December and January, corroborating the observations made by (Vijayakumar et al., 2021).

When assessing models for precipitation, T_{max}, and T_{min} predictions, Fbprophet and SARIMAX consistently showed strong performances, with higher R^2 and NSE values, indicating superior predictive capability. They also exhibited lower P-bias values, indicating reduced bias. While LSTM RNN had competitive results, its NSE values were comparatively lower. Overall, Fbprophet and SARIMAX proved favorable for all three parameters due to their robust performance across multiple evaluation metrics. Limitations include uncertainties in historical data, socioeconomic indicators, and parameter choices for model outputs, as well as unpredictable trajectories in representative concentration pathways (RCPs) and uncertainties in the effectiveness of future climate policies.

7. Conclusions

In conclusion, the examination of historical data using four time-based machine learning models offers valuable insights into projected climate changes in the lower Mahanadi Basin. While total precipitation may not experience a significant change, the distribution across seasons is expected to shift notably. Analysis across various climate scenarios (RCP 2.6, RCP 4.5, and RCP 8.5) indicates consistent trends of increasing annual temperatures over three analyzed periods, with coastal areas experiencing minor fluctuations compared to more significant shifts in the interior and western regions. The predicted precipitation changes suggest an overall increase annually, with diverse patterns in distribution across

the scenarios. Furthermore, the study highlights that the highest annual temperatures are projected to surpass historical records, particularly affecting interior and western areas. Fbprophet and SARIMAX have emerged as superior models for predicting precipitation, T_{max}, and T_{min}, demonstrating strong performance with higher R^2 and NSE values and lower P-bias values, despite limitations such as uncertainties in historical data, socio-economic indicators, and future climate trajectories. In light of these findings, it is evident that the lower Mahanadi Basin faces complex challenges from climate change, necessitating ongoing research and adaptive strategies. Understanding the nuances of precipitation patterns and temperature variations is crucial for effective planning and mitigation efforts. However, uncertainties surrounding future climate policies and trajectories underscore the need for continued monitoring and flexibility in adaptation strategies. Overall, this study underscores the importance of proactive measures to address the potential impacts of climate change on the lower Mahanadi Basin and emphasizes the role of robust modelling techniques in informing decision-making processes.

Acknowledgements

The authors extend their sincere gratitude to the editor and anonymous reviewers for their invaluable insights and dedicated efforts in enhancing the quality of our manuscript. Their thoughtful comments and constructive feedback have greatly contributed to their improvement.

Funding

No funding was obtained for this study.

Author contributions

Gopikrishnan T. conceived the idea, conducted background research, and provided research supervision. Deepak Kumar Raj contributed to data collection, workflow development, and assessment, and led the writing process of the manuscript, with both authors contributing to its composition.

Competing interests

All authors declare that they have no conflicts of interest.

Data availability statement

Precipitation and temperature data for the Mahanadi River basin were obtained from the India Meteorological Department (IMD) (https://www.imdpune.gov.in/; https://swat.tamu.edu/data/india-dataset/).

The CORDEX-SMHI-MIROC-5 Regional Climate Model output was obtained for this study from the Climate4impact website (https://climate4impact.eu/impactportal/general/index.jsp).

Ethics approval

This article does not involve studies with human participants or animals conducted by any of the authors. No ethics approval was needed.

Consent to participate

All contributors to the design of this manuscript willingly provided their consent for its submission.

Consent for publication

All authors have given their consent to publish this manuscript.

References

Alam, M. A., Hossain, S. M., Chanda, Di., & Kabir, M. A. (2021). Performance analysis of LSTMs and Fbprophet models for short term load forecasting. In *2021 5th International Conference on Electrical Engineering and Information and Communication Technology, ICEEICT* (pp. 1–5), Dhaka, Bangladesh. https://doi.org/10.1109/ICEEICT53905.2021.9667833

Almazrouee, A. I., Almeshal, A. M., & Almutairi, A. S. (2020). Long-term forecasting of electrical loads in Kuwait. *Applied Science*, *10*, Article 5627. https://doi.org/10.3390/app10165627

Chaturvedi, S., Rajasekar, E., Natarajan, S., & McCullen, N. (2022). A comparative assessment of SARIMA, LSTM RNN and Fb Prophet models to forecast total and peak monthly energy demand for India. *Energy Policy*, *168*, Article 113097. https://doi.org/10.1016/j.enpol.2022.113097

Dadhwal, V. K., Mahendran, A., Sharma, J. R., Tembhurney, W. M., Joseph, M., Jain, R. K., Singh, H., Paithankar, Y., Manasa Devi, B., & Kalsi, A. P. (2014). *Mahanadi Basin*. https://indiawris.gov.in/downloads/Mahanadi%20Basin.pdf

Das, P., Zhang, Z., & Ren, H. (2022). Evaluation of four bias correction methods and random forest model for climate change projection in the Mara River Basin, East Africa. *Journal of Water and Climate Change*, *13*(4), 1900–1919. https://doi.org/10.2166/wcc.2022.299

Déandreis, C., Pagé, C., Braconnot, P., Bärring, L., Bucchignani, E., de Cerff, W. S., Hutjes, R., Joussaume, S., Mares, C., Planton, S., & Plieger, M. (2014). Towards a dedicated impact portal to bridge the gap between the impact and climate communities: Lessons from use cases. *Climatic Change*, *125*(3–4), 333–347. https://doi.org/10.1007/s10584-014-1139-7

Dhamodharavadhani, S., & Rathipriya, R. (2019). Region-wise rainfall prediction using mapreduce-based exponential smoothing techniques. *Advances in Intelligent Systems and Computing*, *750*, 229–239. https://doi.org/10.1007/978-981-13-1882-5_21

Fadnavis, S., Mahajan, A. S., Choudhury, A. D., Roy, C., Singh, M., & Biswas, M. S. (2020). Atmospheric aerosols and trace gases. In *Assessment of climate change over the Indian region: A report of the Ministry of Earth Sciences (MoES), Government of India* (pp. 93–116). Springer. https://doi.org/10.1007/978-981-15-4327-2_5

Fiseha, B. M., Setegn, S. G., Melesse, A. M., Volpi, E., & Fiori, A. (2014). Impact of climate change on the hydrology of Upper Tiber River basin using bias corrected regional climate model. *Water Resources Management*, *28*(5), 1327–1343. https://doi.org/10.1007/s11269-014-0546-x

Graham, A., Pathak Mishra, E., & Anosh Graham, C. (2017). Time series analysis model to forecast rainfall for Allahabad region. *~ 1418 ~ Journal of Pharmacognosy and Phytochemistry*, *6*(5), 1418–1421.

Haq, M. A. (2022). CDLSTM: A novel model for climate change forecasting. *Computers, Materials and Continua*, *71*(2), 2363–2381. https://doi.org/10.32604/cmc.2022.023059

Ines, A. V. M., & Hansen, J. W. (2006). Bias correction of daily GCM rainfall for crop simulation studies. *Agricultural and Forest Meteorology*, *138*(1–4), 44–53. https://doi.org/10.1016/j.agrformet.2006.03.009

Intergovernmental Panel on Climate Change. (2022). *Impacts, adaptation, and vulnerability: Working group II contribution to the IPCC sixth assessment report of the intergovernmental panel on climate change*. Cambridge University Press. https://doi.org/10.1017/9781009325844

IS-ENES3 C4I-Search. (n.d.). *Welcome to Climate4Impact!* Retrieved January 19, 2024, from https://www.climate4impact.eu/c4i-frontend/

Ishida, K., Kiyama, M., Ercan, A., Amagasaki, M., & Tu, T. (2021). Multi-time-scale input approaches for hourly-scale rainfall–runoff modeling based on recurrent neural networks. *Journal of Hydroinformatics*, *23*(6), 1312–1324. https://doi.org/10.2166/hydro.2021.095

Jain, S., Salunke, P., Mishra, S. K., & Sahany, S. (2019). Performance of CMIP5 models in the simulation of Indian summer monsoon. *Theoretical and Applied Climatology*, *137*(1–2), 1429–1447. https://doi.org/10.1007/s00704-018-2674-3

Jose, D. M., Vincent, A. M., & Dwarakish, G. S. (2022). Improving multiple model ensemble predictions of daily precipitation and temperature through machine learning techniques. *Scientific Reports*, *12*(1), 1–25. https://doi.org/10.1038/s41598-022-08786-w

Kannan, S., & Ghosh, S. (2011). Prediction of daily rainfall state in a river basin using statistical downscaling from GCM output. *Stochastic Environmental Research and Risk Assessment*, *25*(4), 457–474. https://doi.org/10.1007/s00477-010-0415-y

Khan, M. M. R., Siddique, M. A. B., Sakib, S., Aziz, A., Tasawar, I. K., & Hossain, Z. (2020). Prediction of temperature and rainfall in Bangladesh using long short term memory recurrent neural networks. In *2020 4th International Symposium on Multidisciplinary Studies and Innovative Technologies* (pp. 1–6), Istanbul, Turkey. https://doi.org/10.1109/ISMSIT50672.2020.9254585

Krishna Kumar, K., Patwardhan, S. K., Kulkarni, A., Kamala, K., Koteswara Rao, K., & Jones, R. (2011). Simulated projections for summer monsoon climate over India by a high-resolution regional climate model (PRECIS). *Current Science*, *101*(3), 312–326.

Mavume, A. F., Banze, B. E., Macie, O. A., & Queface, A. J. (2021). Analysis of climate change projections for mozambique under the representative concentration pathways. *Atmosphere*, *12*(5), Article 588. https://doi.org/10.3390/atmos12050588

McHugh, C., Coleman, S., Kerr, D., & McGlynn, D. (2019). Forecasting day-ahead electricity prices with a SARIMAX model. In *2019 IEEE Symposium Series on Computational Intelligence* (pp. 1523–1529), Xiamen, China. https://doi.org/10.1109/SSCI44817.2019.9002930

Mujumdar, P. P., & Ghosh, S. (2008). Modeling GCM and scenario uncertainty using a possibilistic approach: Application to the Mahanadi River, India. *Water Resources Research*, *44*(6), 1–15. https://doi.org/10.1029/2007WR006137

Pattanaik, D. R., & Das, A. K. (2015). Prospect of application of extended range forecast in water resource management: A case study over the Mahanadi River basin. *Natural Hazards*, *77*(2), 575–595. https://doi.org/10.1007/s11069-015-1610-4

Perkins, S. E., Moise, A., Whetton, P., & Katzfey, J. (2014). Regional changes of climate extremes over Australia – A comparison of regional dynamical downscaling and global climate model simulations. *International Journal of Climatology*, *34*(12), 3456–3478. https://doi.org/10.1002/joc.3927

Rathjens, H., Bieger, K., Srinivasan, R., & Arnold, J. G. (2016). *CMhyd user manual: Documentation for preparing simulated climate change data for hydrologic impact studies*. https://swat.tamu.edu/media/115265/bias_cor_man.pdf

Rohini, P., Rajeevan, M., & Mukhopadhay, P. (2019). Future projections of heat waves over India from CMIP5 models. *Climate Dynamics*, *53*(1), 975–988. https://doi.org/10.1007/s00382-019-04700-9

Salvi, K., Villarini, G., Vecchi, G. A., & Ghosh, S. (2017). Decadal temperature predictions over the continental United States: Analysis and enhancement. *Climate Dynamics*, *49*(9–10), 3587–3604. https://doi.org/10.1007/s00382-017-3532-1

Saranya, M. S., & Vinish, V. N. (2021). Evaluation and selection of CORDEX-SA datasets and bias correction methods for a hydrological impact study in a humid tropical river basin, Kerala. *Journal of Water and Climate Change*, *12*(8), 3688–3713. https://doi.org/10.2166/wcc.2021.139

Selvin, S., Vinayakumar, R., Gopalakrishnan, E. A., Menon, V. K., & Soman, K. P. (2017). Stock price prediction using LSTM, RNN and CNN-sliding window model. In *2017 International Conference on Advances in Computing, Communications and Informatics* (pp. 1643–1647), Udupi, India. https://doi.org/10.1109/ICACCI.2017.8126078

Swain, S. (2016). *Impact of climate variability over Mahanadi River Basin*.

Teutschbein, C., & Seibert, J. (2012). Bias correction of regional climate model simulations for hydrological climate-change impact studies: Review and evaluation of different methods. *Journal of Hydrology*, *456–457*, 12–29. https://doi.org/10.1016/j.jhydrol.2012.05.052

Tsai, Y. T., Zeng, Y. R., & Chang, Y. S. (2018). Air pollution forecasting using RNN with LSTM. In *2018 IEEE 16th International Conference on Dependable, Autonomic and Secure Computing, IEEE 16th International Conference on Pervasive Intelligence and Computing, IEEE 4th International Conference on Big Data Intelligence and Computing and Cyber Science and Technology Congress* (pp. 1074–1079), Athens, Greece. https://doi.org/10.1109/DASC/PiCom/DataCom/CyberSciTec.2018.00178

Vagropoulos, S. I., Chouliaras, G. I., Kardakos, E. G., Simoglou, C. K., & Bakirtzis, A. G. (2016). Comparison of SARIMAX, SARIMA, modified SARIMA and ANN-based models for short-term PV generation forecasting. In *2016 IEEE International Energy Conference* (pp. 1–6), Leuven, Belgium. https://doi.org/10.1109/ENERGYCON.2016.7514029

Vijayakumar, S., Nayak, A. K., Ramaraj, A. P., Swain, C. K., Geethalakshmi, V., Pazhanivelan, S., Tripathi, R., & Sudarmanian, N. S. (2021). Rainfall and temperature projections and their impact assessment using CMIP5 models under different RCP scenarios for the eastern coastal region of India. *Current Science*, *121*(2), 222–232. https://doi.org/10.18520/cs/v121/i2/222-232

Yeboah, K. A., Akpoti, K., Kabo-bah, A. T., Ofosu, E. A., Siabi, E. K., Mortey, E. M., & Okyereh, S. A. (2022). Assessing climate change projections in the Volta Basin using the CORDEX-Africa climate simulations and statistical bias-correction. *Environmental Challenges*, *6*, Article 100439. https://doi.org/10.1016/j.envc.2021.100439